Nanotechnology

PAPER

Reduction of dislocation, mean free path, and migration barriers using high entropy alloy: insights from the atomistic study of irradiation damage of CoNiCrFeMn

To cite this article: Yangen Li *et al* 2020 *Nanotechnology* **31** 425701

IOP Publishing Nanotechnology

Nanotechnology **31** (2020) 425701 (8pp) https://doi.org/10.1088/1361-6528/ab9cf5

Reduction of dislocation, mean free path, and migration barriers using high entropy alloy: insights from the atomistic study of irradiation damage of CoNiCrFeMn

Yangen Li[1], Rui Li[1], Qing Peng[2] and Shigenobu Ogata[3]

[1] School of Mechanical Engineering, University of Science and Technology Beijing, Beijing 100083, People's Republic of China
[2] Physics Department, King Fahd University of Petroleum and Minerals, Dhahran 31261, Saudi Arabia
[3] Department of Mechanical Science and Bioengineering, Osaka University, Osaka 560-8531, Japan

E-mail: lirui@ustb.edu.cn and qpeng.org@gmail.com

Received 17 February 2020, revised 5 June 2020
Accepted for publication 15 June 2020
Published 23 July 2020

Abstract

High entropy alloy has attracted extensive attention in nuclear energy due to outstanding irradiation resistance, partially due to sluggish diffusion. The mechanism from a defect-generation perspective, however, has received much less attention. In this paper, the formation of dislocation loops, and migration of interstitials and vacancies in CoNiCrFeMn high entropy alloy under consecutive bombardments were studied by molecular dynamics simulations. Compared to pure Ni, less defects were produced in the CoNiCrFeMn. Only a few small dislocation loops were observed, and the length of dislocation was small. The dislocation loops in Ni matrix were obviously longer and so was the length of dislocation. The interstitial clusters had much smaller mean free path during migration in the CoNiCrFeMn. The mean free path of 10-interstitial clusters in CoNiCrFeMn was reduced over 40 times compared to that in pure Ni. In addition, CoNiCrFeMn had a smaller difference of migration energy between interstitial and vacancy, which increased the opportunity of recombination of defects, therefore, led to less defects and much fewer dislocation loops. Our results provide insights into the mechanism of irradiation resistance in the high entropy alloy and could be useful in material design for irradiation tolerance and accident tolerance materials in nuclear energy.

Supplementary material for this article is available online

Keywords: high entropy alloy, irradiation resistance, cascade collision, defects, dislocation loops

(Some figures may appear in colour only in the online journal)

1. Introduction

With the development of next generation nuclear reactors, the working environment of nuclear structural materials becomes more severe, which leads to the failure of some traditional structural materials. There is an urgent need to investigate the irradiation resistance performance of new structural materials under severe working conditions [1, 2]. High entropy alloys (HEAs) are one of the best candidates. Unlike traditional alloys that contain only one or two major elements, HEAs contain several elements that are randomly distributed in equal proportion [3, 4]. The complexity of compositions

in HEAs might enhance irradiation tolerance in severe irradiation environments [5–8]. Hyeon-Seok *et al* [9] characterized the generation and evolution of point defects in HEA, and indicated that defect clusters appearing in the HEA were unstable due to the alloy's complexity. Chen *et al* [10] investigated the diffusion and formation of helium bubbles to validate whether HEA had an excellent helium irradiation resistance performance under helium implantation. Yang *et al* [11] studied the structure and phase stabilities of HEAs under irradiation and explored the microstructure and chemical composition dependence of irradiation tolerances. In addition, researchers results have shown that HEAs had excellent mechanical properties, good ductility at low temperatures as well as high strength at high temperatures and excellent corrosion and wear resistance, which are also beneficial for their potential application [12–18]. Although researchers have done significant work on the irradiation resistance behavior and other properties of HEA, the generation of dislocation loops during consecutive bombardments, the mean free path of defect clusters and migration barriers in HEAs have not been systematically studied, in particular the dynamic behavior of interstitial clusters and vacancy defects have recieved little attention.

Under high temperature and high energy irradiation working conditions, a large number of interstitial atoms and vacancy defects are generated inside the materials [19, 20]. The migration of interstitial clusters decreased the possibility of trapping vacancy defects and annihilation, and the aggregation of vacancies could lead to the collapse of vacancies to form dislocation loops [21, 22], which reduced the stability of structures and shortened the life of materials. Mohammad *et al* [23] studied the effect of chemical alternation on the irradiation resistance. The results showed that increasing the complexity of the alloy led to decreased defect mobility. Lu *et al* [6] indicated that controlling the defect mobility and migration pathways could enhance irradiation tolerance and that the complexity of high entropy alloys allowed it to be a promising anti-irradiation material. Zhao *et al* [24] pointed out that the growth of vacancy clusters could be suppressed by controlling cluster migration pathways and diffusion kinetics. Levo *et al* [22] showed that increasing complexity of alloys did not always decrease the accumulation of damage. The evolution of defects and transformation of dislocation might be the key factor. Therefore, controlling the formation and migration of defects was key to improving the irradiation tolerance of materials [6, 25]. CoNiCrFeMn HEA has attracted extensive attention in nuclear energy due to the potential outstanding irradiation resistance. Lu *et al* [26] indicated that the increased complexity in CoNiCrFeMn HEA could extend the incubation period and delay dislocation loop growth during irradiation. Hyeon-Seok *et al* [9] reported that CoNiCrFeMn HEA had high radiation damage tolerance owing to the alloy complexity. We also studied the enhanced surface bombardment resistance of CoNiCrFeMn HEA under extreme irradiation flux [27]. However, the irradiation damage in the bulk CoNiCrFeMn HEA is still unclear. The dynamic behavior of interstitial clusters and vacancy defects in CoNiCrFeMn HEA under severe working conditions has not received much attention. In this paper, the accumulation and evolution of defects in CoNiCrFeMn HEA under high energy consecutive bombardments at high temperature were studied by molecular dynamics simulation and compared to that of pure Ni. The migration energy of interstitial and vacancy in CoNiCrFeMn high-entropy alloy were calculated and the migration behavior of interstitial clusters and vacancy defects were discussed.

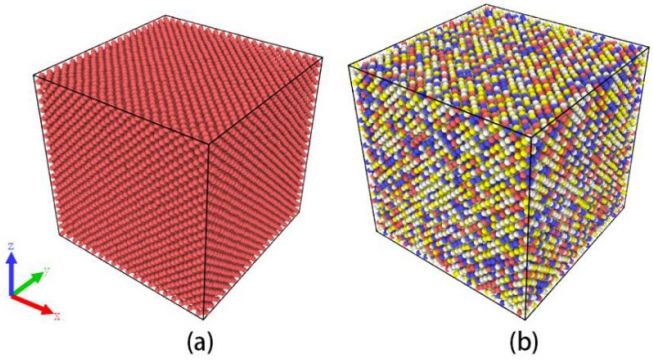

Figure 1. The models of Ni(a) and CoNiCrFeMn HEA(b).

2. Simulation models and method

The Ni and CoNiCrFeMn HEA simulation models are shown in figures 1(a) and (b), respectively. In the Ni model, the number of Ni atoms was 32 000. In the HEA model, five types of atoms in CoNiCrFeMn HEA were equal in proportional and randomly distributed, with the total number of atoms being 32 000. The short-range order (SRO) of a HEA is critical to its physical properties [28], therefore, we calculated the SRO parameters for all possible nearest neighbor bonds to check the randomness of the five different elements. The results showed that five types of atoms in the CoNiCrFeMn could be regarded as a random distribution. More details of the calculation results are presented in the supplementary data files (available online at stacks.iop.org/NANO/31/425701/mmedia). The two models both had a size of 7.06 nm in the x, y, and z directions. Periodic boundary conditions were applied along the x, y and z directions. Cascade collision atoms were chosen in the center of the simulation model with an energy of 3000 eV. The single PKA (primary knock-on atom) process had been taken to confirm that the box was big enough for the energy of 3000 eV. In order to simulate a homogeneous irradiation effect, the simulation model was shifted by a random direction and distance (less than the size of the simulation model) after each cascade collision, all the atoms outside were shifted back using the periodic boundary to keep the model complete. This allowed the random irradiation positions and homogeneous irradiation to be achieved even though all the cascade collision atoms were chosen in the center of the model, this procedure also can be found elsewhere [22, 29]. The temperature at 700 K was adopted to mimic the severe working environment [30]. The consecutive bombardments were carried out 300 time. Large-scale atomic molecular massively parallel simulator (LAMMPS) was used to simulate the whole

continuous cascades collisions process [31]. The OVITO visualization tool was used to observe the trajectories of atoms.

The interatomic interactions among the Co, Ni, Cr, Fe and Mn atoms were described using the 2NN MEAM potential [32]. In addition, as reported by Hyeon-Seok [9], the short-range repulsion was very important in the cascade collisions simulation, the d parameters in unary Co and Mn were adjusted from 0 to 0.03 and 0.02, respectively. Therefore, five types of atoms all had sufficient short-range repulsion during cascade collisions. It has been confirmed that this adjustment had little effect on the physical properties of each unary system. Before the cascade collisions simulation, the matrixes were annealed under isothermal-isobaric (NPT) ensemble with a time step of 0.001 ps. The annealing process was as follows. First, the simulation system was relaxed at 300 K for 100 ps, then was heated to 2000 K at a rate of 3.4 K ps^{-1} and maintained for 1000 ps. Finally, the system cooled to 300 K at a rate of 3.4 K ps^{-1}. The irradiation cascade collision stage was with the micro-canonical (NVE) ensemble, in which an adaptive time step was used so that each atom did not move more than 0.002 nm. A Berendsen thermostat was applied to control the irradiation temperature T = 700 K of the 0.5 nm thick layers at all sides of the matrix to avoid excessive temperature [33]. In addition, the intervals between two adjacent cascade events was 50 ps to allow the temperature of the system cool to about 700 K and ensure defect clusters migration had all finished.

3. Results and discussions

3.1. Point defects generation

For the point defects analysis, the Wigner-Seitz method was used to calculate the sum of defects [34]. The dislocation extraction algorithm (DXA) method was applied to analyze the dislocation distribution in the matrix [35]. As shown in figure 2(a), the number of defects in the Ni matrix rapidly increased to about 300 at the beginning of consecutive bombardments and kept increasing for a long time as the cascade collisions continued. After 300 consecutive series of bombardments, the number of defects reached more than 950. The number of interstitial clusters of different sizes in the Ni matrix after 50, 100, 150, 200, 250 and 300 sets of cascade collisions are shown in figure 2(b). Two obvious phenomena were observed. First, the average number of small size clusters (between 1 and 10) changed significantly, which means that the migration of small size cluster was very active. Second, large sized clusters (more than 51) appeared in the Ni matrix during the whole consecutive bombardments. When the point defects aggregated into large sized clusters, the formation of a large number of dislocation loops might happen [36, 37]. Therefore, this phenomenon indicated that the defects generated by the cascade collisions migrated and aggregated in the Ni matrix. In addition, we also noticed a sharp decrease in the number of defects after 240 sequences of bombardments, which was caused by the absorption of a large number of Shockley 1/6 <112> loops into only one Frank 1/3 <111> loop. Therefore, the matrix structure was partially recovered and the number of defects

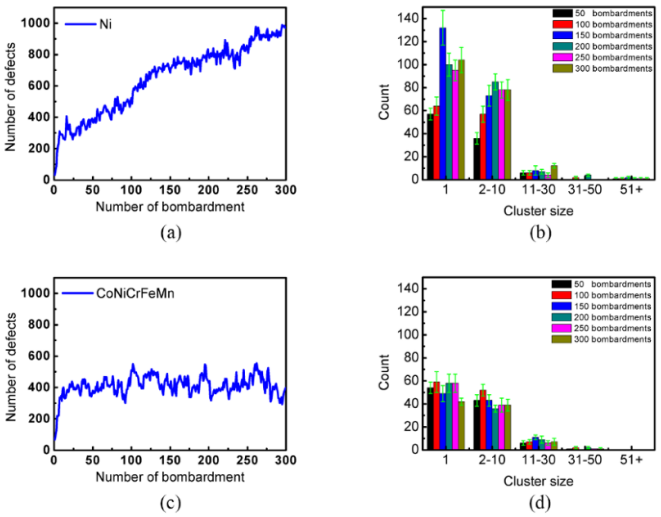

Figure 2. The number of defects in Ni (a) and CoNiCrFeMn HEA (c) during 300 times of consecutive bombardments. The number of interstitial clusters in different size in Ni matrix (b) and CoNiCrFeMn HEA (d) after 50, 100, 150, 200, 250 and 300 times of consecutive bombardments.

decreased. All the dislocation loops were analyzed using the DXA method and the details can be seen in supplementary movie 1. The number of defects in the CoNiCrFeMn HEA are shown in figure 2(c), which represented obviously different trends form the Ni matrix. The number of defects remained stable during the whole cascade collision process. The total number was around 400, which was smaller than the value in the Ni matrix after 300 consecutive bombardments. Moreover, the interstitial clusters of different sizes between the Ni and CoNiCrFeMn HEA was also quite different. The number of interstitial clusters of different sizes in CoNiCrFeMn HEA after 50, 100, 150, 200, 250 and 300 series of cascade collisions is shown in figure 2(d). The interstitial clusters were mainly of a small size (between 1 and 10), and there was no obvious change in the distribution of defect cluster size during the consecutive bombardments, which implied that the defects in CoNiCrFeMn HEA were latively dispersed and no large scale migration and aggregation occurred. The different behavior of CoNiCrFeMn HEA compared to Ni matrix was attributed to the lattice distortion effect of the HEA [38, 39], which could successfully suppress the migration of defects and promote the recombination of interstitials and vacancies. Our previous works on surface bombardment showed a similar trend with the bombardment in the middle [27]. The number of defects increased rapidly in Ni, and the generation of defects in HEA was slow and stable. The difference in defects between Ni and HEA could also be found in other simulations and experimental works [22, 40].

3.2. Dislocation loops generation

Figures 3 and 4 show the evolution of dislocation loops in Ni and CoNiCrFeMn HEA, respectively, after 50, 100, 150, 200, 250, 300 consecutive bombardments. In the Ni matrix, a large number of dislocation loops formed during continuous cascade collisions. The Frank 1/3 <111> loop kept growing

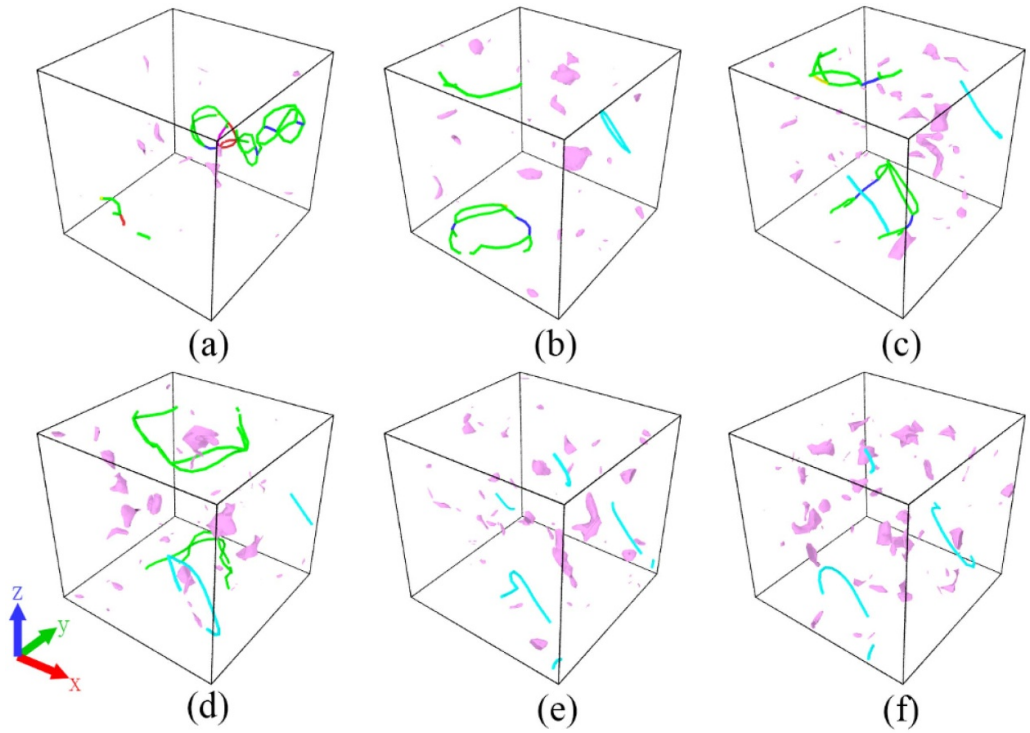

Figure 3. Distribution of defects and dislocation loops in Ni matrix. (a)-(f) was the distribution after 50, 100, 150, 200, 250, 300 times of consecutive bombardments, respectively. The lines with different colors represented different types of dislocation loops, where blue, green, purple, yellow, light blue denoted the Perfect 1/2 < 110 >, Shockley 1/6 < 112 >, Srair-rod 1/6 < 110 >, Hirth 1/3 < 001 >, Frank 1/3 < 111 > dislocation loops respectively. Red lines were the dislocation loops that could not be identified by DXA. The pink meshes were the defects meshes.

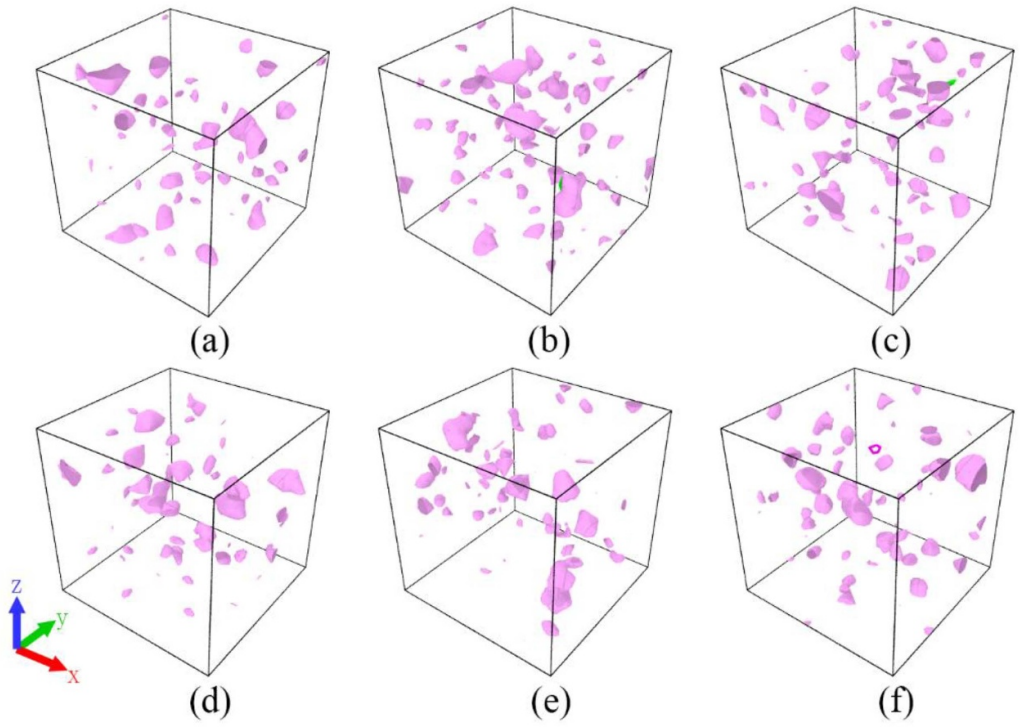

Figure 4. Distribution of defects and dislocation loops in the CoNiCrFeMn HEA. (a)-(f) was the distribution after 50, 100, 150, 200, 250, 300 times of consecutive bombardments, respectively. The colors of lines or meshes indicated the same with figure 3

during the whole process. After 300 sets of consecutive collisions, long length dislocation loops remained in the Ni matrix. However, in CoNiCrFeMn HEA, as shown in figure 4, most of the defects existed in the form of small clusters.

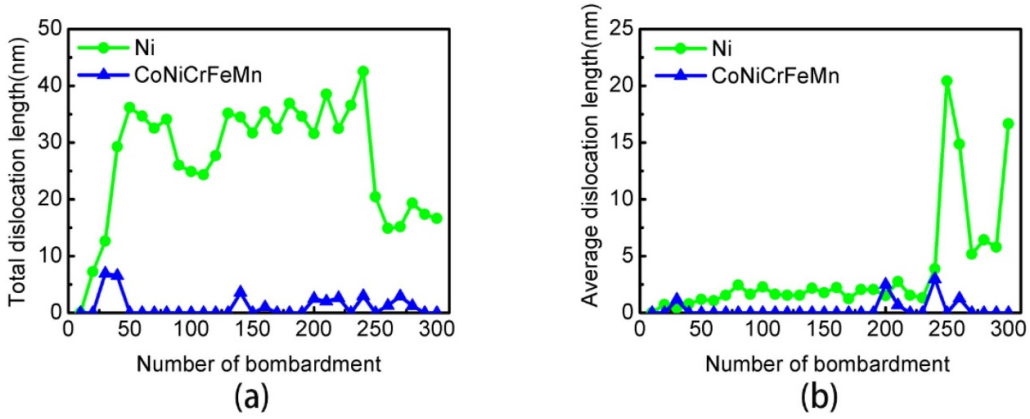

Figure 5. Statistics of dislocation loops in Ni and CoNiCrFeMn HEA during 300 times of consecutive bombardments. (a) was the total dislocation length, (b) was the average dislocation length.

Defects were rarely observed to form dislocation loops during the whole collision process. Our previous study on surface bombardment also showed that the existence of dislocation loops was seldom observed in CoNiCrFeMn HEA. The result indicates that the defects in Ni matrix more easily aggregated and collapsed to form dislocation loops, while the formation and growth of dislocation loops in the HEA were significantly suppressed.

To further analyze the defects and dislocation loops during consecutive bombardments, the total length of dislocation and the average length of dislocation loops in Ni and CoNiCrFeMn HEA were calculated, respectively. In the Ni matrix, the total dislocation length is shown in figure 5(a), large number of dislocation loops form in the beginning stage of consecutive bombardments. The total dislocation length remained at a high level during most time of the consecutive cascade collisions and reached more than 40 nm. Finally, because of the absorption of dislocation loops, only one big Frank 1/3 <111> loop existed, and the total length was 20 nm. The average length of dislocation loops was stable and remained at a relatively low level during most of the consecutive cascade collisions, as shown in figure 5(b). However, with the absorption and combining of dislocation loops, the average length of dislocation loops finally reached more than 18 nm, and the size of dislocation loops was significantly larger. As for CoNiCrFeMn HEA, the growth of dislocation loops was suppressed during the whole collision process. The total dislocation length and the average dislocation length both remained at a very low level. Some researchers [6, 9] indicated that the lattice distortion due to the alloy complexity could lead to high recombination of defects and therefore the size of the dislocation loops become significantly smaller, which was consistent with our simulation results.

3.3. Mean free path

It has been demonstrated that small defect clusters in metal materials could migrate along the close-packed row of atoms [41, 42]. For simple metals, small interstitial clusters could migrate rapidly through 1D motion [43, 44]. When the compositional complexity of material increased, the cluster migration mode was affected, and the transition from 1D to 3D motion might occur. Mean free path (MFP) was applied to evaluate the migration behavior of clusters in Ni and CoNiCrFeMn HEA. The mean free path was determined by calculating the average migration distance of the small defect clusters before they changed migration direction. In order to study the migration behavior of interstitial clusters in Ni and CoNiCrFeMn HEA, a small interstitial cluster was created by inserting atoms inside the matrix. To make each element have a good chance to be presented in the interstitial cluster and considering our results about the number of interstitial clusters of different sizes in figure 2, we chose a 10-atom cluster as a compromise for the computing demands and representatives.

Since the internal temperature of the matrix would reach a high temperature of about 1200 K during cascades collisions, simulations with a temperature 1200 K were conducted. The migration trajectories of the center of interstitial cluster in Ni and CoNiCrFeMn HEA are shown in figures 6(a) and (b), respectively. The results show that the interstitial cluster in the Ni matrix migrated a long distance with 1D motion with relatively large mean free path before changing the direction of motion. However, for the interstitial cluster in the HEA, only a vibration in 3D within a small range was observed, with a much lower MFP, which was consistent with previous experimental work [6]. The MFP of Ni and CoNiCrFeMn HEA was over 40 nm and less than 1 nm, respectively. The detailed migration behavior of the interstitial cluster in Ni and CoNiCrFeMn HEA can be seen in supplementary movies 2 and 3. The MFP of 10-interstitial clusters in CoNiCrFeMn has been reduced over 40 times compared to that in pure Ni, which might be a key mechanism for the high irradiation tolerance of CoNiCrFeMn high entropy alloy.

A cage model could be used to explain the sluggish diffusion of HEA which caused the different migration behavior of defect clusters between Ni and CoNiCrFeMn HEA [25]. For traditional binary alloys, the minor element was randomly distributed on lattice sites. The percentage of minor element was assumed as c (where $0 < c < 50\%$). These minor element atoms could be seen as forming many cages and restricted

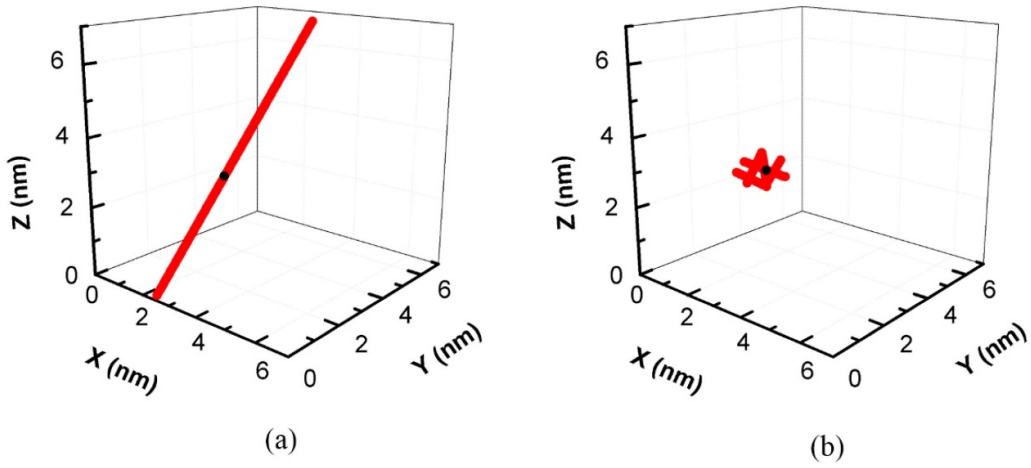

Figure 6. The trajectories of a ten interstitials cluster in Ni (a) and CoNiCrFeMn HEA (b). The MFP of Ni and CoNiCrFeMn HEA was over 40 nm and less than 1 nm, respectively.

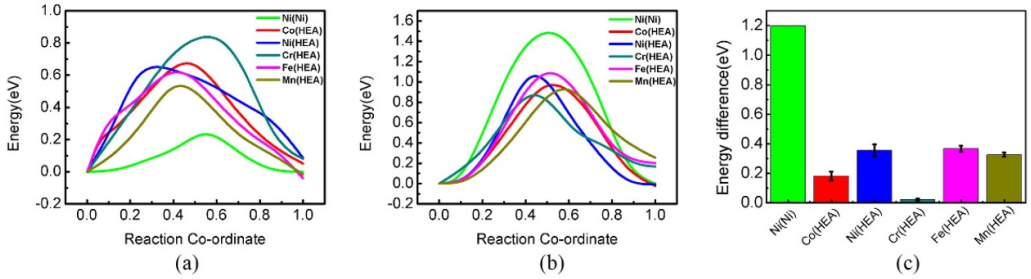

Figure 7. (a) Interstitial and (b) vacancy migration energy in Ni and CoNiCrFeMn HEA. (c) The difference of interstitial and vacancy migration energy in Ni and CoNiCrFeMn HEA.

the movement of defects in these cage regions. The interstitial clusters migrate via 1D motion within one cage, however, the migration motion changed and gradually tended to 3D motion on the surface or edge of the cage. The mean free path (MFP) λ in the cage model was a formula related to the minor element percentage of c, where A and B are constants for fitting to the MFP formula.

$$\lambda = \mathrm{A}c^{-\frac{1}{3}} + B \tag{1}$$

According to the formula, the MFP decreased with the increasing of the percentage of minor element. For traditional binary alloys, c was less than 50%. However, for CoNiCrFeMn HEA that contained five main elements in equal proportions and maintained a complete atom lattice, the corresponding minor element percentage c extended to 80% for each element, which suppressed the migration of the interstitial clusters and dislocations more obviously, therefore, the MFP of the CoNiCrFeMn HEA was significantly smaller.

The migration behavior of interstitial behavior caused the difference of defects and dislocation loops between Ni and CoNiCrFeMn HEA. When the interstitial clusters in the Ni matrix migrated a long distance via 1D motion, they would be out of the cascade region, therefore, the probability for the interstitial clusters to recombine with vacancies would be greatly reduced, and thus more defects remained. Moreover, when the interstitial cluster migrated rapidly from the cascade region to the surface or the inside of Ni matrix, the local supersaturation of material was aggravated, which would result in severe swelling and the formation of dislocation loops [45, 46]. As reported by previous works [6, 25], the high lattice distortion of HEA not only suppressed the migration of interstitial clusters, but also enhanced the probability of recombination of interstitials and vacancies through local vibration. Therefore, compared with Ni, the compositional complexity of CoNiCrFeMn HEA enhanced irradiation resistance.

3.4. Migration barrier

As we reported in section 3.3, the migration behavior of defects had important influence on the irradiation resistance performance. Therefore, single interstitial and vacancy migration energy of Ni and CoNiCrFeMn HEA were also calculated in this paper. The migration energy was calculated by using the NEB method [47, 48]. With this method, after defining initial and final structures with interstitial or vacancy, the change of the total energy during the migration path was calculated, then the interstitial and vacancy migration energy was determined by calculating the climbing barrier of the model. As shown in figures 7(a) and (b), the average interstitial migration energies of Ni and CoNiCrFeMn HEA were 0.28 eV and 0.71 eV, respectively, and the average vacancy migration energies of Ni and CoNiCrFeMn HEA were 1.48 eV and 0.97 eV, respectively. It should be observed that the difference in the

interstitial and vacancy migration energy of Ni and HEA was quite different. Figure 7(c) showed the migration energy difference between vacancy and interstitial, the interstitial and vacancy of HEA had similar migration energy, and the average difference was within 0.26 eV, while the migration energy of vacancy was much larger than interstitial in Ni, and the difference was more than 1.2 eV. In addition, the migration energy could be uniquely defined in pure Ni, but not in the HEA due to the compositional complexity. Therefore, multiple simulations were carried out to obtain the average value of HEA. Our results showed that vacancy and interstitial of HEA had similar mobility, which implied that the synchronization of interstitial and vacancy migration could increase the probability of recombination [6]. As for Ni, the migration energy of vacancy was significantly larger than interstitial. Interstitials would escape rapidly from the cascade region, resulting in a large number of vacancies remaining in the Ni matrix, and the aggregation and collapse of vacancies would lead to the formation of dislocation loops. Therefore, the difference in the interstitial and vacancy migration energy of Ni and CoNiCrFeMn HEA may be the key factor for the radiation resistance.

4. Conclusion

In this paper, consecutive bombardments to Ni and CoNiCrFeMn HEA were conducted by molecular dynamics simulation. The results showed that more defects occurred in the Ni matrix and that the defects tended to form large size dislocation loops. However, defects in CoNiCrFeMn HEA existed in the form of small clusters, and the formation of dislocation loops could be effectively suppressed. The MFP was analyzed to compare the migration behavior of interstitial clusters in Ni and CoNiCrFeMn HEA. The results showed that high level lattice distortion and sluggish diffusion of CoNiCrFeMn HEA led to the 3D vibration of interstitial clusters in a small range, therefore, the migration of interstitial defects was greatly suppressed, which increased the probability of being trapped and annihilated by the vacancies. The cage model was used to explain the sluggish diffusion of CoNiCrFeMn HEA. Because the percentage of minor elements could extend to 80%, the MFP of CoNiCrFeMn HEA was significantly smaller. In addition, interstitials and vacancies in CoNiCrFeMn HEA had similar mobility, which led to the higher recombination rate. In contrast, interstitials migrated faster than vacancies in the Ni matrix, resulting in a large number of vacancies remaining, and dislocation loops formed more easily. In summary, our results showed that CoNiCrFeMn HEA performed obviously better than the Ni matrix under consecutive bombardments and the mechanism of irradiation resistance in the HEA were also explained. Excellent irradiation resistance performance of CoNiCrFeMn HEA could be expected in its application for next generation nuclear reactors.

Acknowledgments

The work is supported by the National Natural Science Foundation of China (No. 51475039). Q Peng would like to acknowledge the support provided by the Deanship of Scientific Research (DSR) at King Fahd University of Petroleum & Minerals (KFUPM) for funding this work through project No. SR191013.

ORCID iDs

Rui Li https://orcid.org/0000-0003-0258-281X
Qing Peng https://orcid.org/0000-0002-8281-8636
Shigenobu Ogata https://orcid.org/0000-0002-9072-4496

References

[1] Budnitz R J 2016 Nuclear power: status report and future prospects *Energy Policy* **96** 735–9
[2] Zinkle S J and Snead L L 2014 Designing radiation resistance in materials for fusion energy *Annu. Rev. Mater. Res.* **44** 241–67
[3] Santodonato L J, Zhang Y, Feygenson M, Parish C M, Gao M C, Weber R J, Neuefeind J C, Tang Z and Liaw P K 2015 Deviation from high-entropy configurations in the atomic distributions of a multi-principal-element alloy *Nat. Commun.* **6** 5964
[4] Jin K, Sales B C, Stocks G M, Samolyuk G D, Daene M, Weber W J, Zhang Y and Bei H 2016 Tailoring the physical properties of Ni-based single-phase equiatomic alloys by modifying the chemical complexity *Sci. Rep.* **6** 20159
[5] Sheng G and Liu C T 2011 Phase stability in high entropy alloys: formation of solid-solution phase or amorphous phase *Prog. Nat. Sci.* **21** 433–46
[6] Lu C, Niu L, Chen N, Jin K, Yang T, Xiu P, Zhang Y, Gao F, Bei H and Shi S 2016 Enhancing radiation tolerance by controlling defect mobility and migration pathways in multicomponent single-phase alloys *Nat. Commun.* **7** 13564
[7] He M-R, Wang S, Shi S, Jin K, Bei H, Yasuda K, Matsumura S, Higashida K and Robertson I M 2017 Mechanisms of radiation-induced segregation in CrFeCoNi-based single-phase concentrated solid solution alloys *Acta. Mater.* **126** 182–93
[8] Granberg F, Nordlund K, Ullah M W, Jin K, Lu C, Bei H, Wang L, Djurabekova F, Weber W and Zhang Y 2016 Mechanism of radiation damage reduction in equiatomic multicomponent single phase alloys *Phys. Rev. Lett.* **116** 135504
[9] Do H-S and Lee B-J 2018 Origin of radiation resistance in multi-principal element alloys *Sci. Rep.* **8** 16015
[10] Chen D, Tong Y, Li H, Wang J, Zhao Y L, Hu A and Kai J J 2018 Helium accumulation and bubble formation in FeCoNiCr alloy under high fluence He+ implantation *J. Nucl. Mater.* **501** 208–16
[11] Chen F, Tang X, Yang Y, Huang H, Liu J, Li H and Chen D 2016 Atomic simulations of Fe/Ni multilayer nanocomposites on the radiation damage resistance *J. Nucl. Mater.* **468** 164–70
[12] Yeh J W, Chen S K, Lin S J, Gan J Y, Chin T S, Shun T T, Tsau C H and Chang S Y 2004 Nanostructured high-entropy alloys with multiple principal elements: novel alloy design concepts and outcomes *Adv. Eng. Mater.* **6** 299–303
[13] Tsai M-H 2013 Physical properties of high entropy alloys *Entropy* **15** 5338–45
[14] Tong C-J, Chen Y-L, Yeh J-W, Lin S-J, Chen S-K, Shun -T-T, Tsau C-H and Chang S-Y 2005 Microstructure characterization of Al x CoCrCuFeNi high-entropy alloy

system with multiprincipal elements *Metall. Mater. Trans.* A **36** 881–93
[15] Li Z, Pradeep K G, Deng Y, Raabe D and Tasan C C 2016 Metastable high-entropy dual-phase alloys overcome the strength–ductility trade-off *Nature* **534** 227
[16] Gludovatz B, Hohenwarter A, Catoor D, Chang E H, George E P and Ritchie R O 2014 A fracture-resistant high-entropy alloy for cryogenic applications *Science* **345** 1153–8
[17] Wu Z, Bei H, Pharr G M and George E P 2014 Temperature dependence of the mechanical properties of equiatomic solid solution alloys with face-centered cubic crystal structures *Acta. Mater.* **81** 428–41
[18] Ding Q, Zhang Y, Chen X, Fu X, Chen D, Chen S, Gu L, Wei F, Bei H and Gao Y 2019 Tuning element distribution, structure and properties by composition in high-entropy alloys *Nature* **574** 223–7
[19] Rong F C and Watkins G 1986 ODMR observation of close frenkel pairs in electron-irradiated ZnSe *Mater. Sci. Forum* **10** 827–32
[20] Nordlund K, Ghaly M, Averback R, Caturla M, de La Rubia T D and Tarus J 1998 Defect production in collision cascades in elemental semiconductors and fcc metals *Phys. Rev.* B **57** 7556
[21] Peng Q, Meng F, Yang Y, Lu C, Deng H, Wang L, De S and Gao F 2018 Shockwave generates< 100> dislocation loops in bcc iron *Nat. Commun.* **9** 4880
[22] Levo E, Granberg F, Fridlund C, Nordlund K and Djurabekova F 2017 Radiation damage buildup and dislocation evolution in Ni and equiatomic multicomponent Ni-based alloys *J. Nucl. Mater.* **490** 323–32
[23] Ullah M W, Xue H, Velisa G, Jin K, Bei H, Weber W J and Zhang Y 2017 Effects of chemical alternation on damage accumulation in concentrated solid-solution alloys *Sci. Rep.* **7** 4146
[24] Zhao S J, Velisa G, Xue H Z, Bei H B, Weber W J and Zhang Y W 2017 Suppression of vacancy cluster growth in concentrated solid solution alloys *Acta. Mater.* **125** 231–7
[25] Lu C, Yang T, Niu L, Peng Q, Jin K, Crespillo M L, Velisa G, Xue H, Zhang F and Xiu P 2018 Interstitial migration behavior and defect evolution in ion irradiated pure nickel and Ni-xFe binary alloys *J. Nucl. Mater.* **509** 237–44
[26] Lu C *et al* 2017 Radiation-induced segregation on defect clusters in single-phase concentrated solid-solution alloys *Acta. Mater.* **127** 98–107
[27] Li Y, Li R and Peng Q 2019 Enhanced surface bombardment resistance of the CoNiCrFeMn high entropy alloy under extreme irradiation flux *Nanotechnology* 10.1088/1361-6528/ab473f
[28] Fernández-Caballero A, Fedorov M, Wróbel J S, Mummery P M and Nguyen-Manh D 2019 Configurational entropy in multicomponent alloys: matrix formulation from Ab initio based hamiltonian and application to the FCC Cr-Fe-Mn-Ni system *Entropy* **21** 68
[29] Ullah M W, Aidhy D S, Zhang Y and Weber W J 2016 Damage accumulation in ion-irradiated Ni-based concentrated solid-solution alloys *Acta. Mater.* **109** 17–22
[30] Guérin Y, Was G S and Zinkle S J 2009 Materials challenges for advanced nuclear energy systems *MRS Bull.* **34** 10–19
[31] Plimpton S 1995 Fast parallel algorithms for short-range molecular dynamics *J. Comput. Phys.* **117** 1–19
[32] Choi W M, Jo Y H, Sohn S S, Lee S and Lee B J 2018 Understanding the physical metallurgy of the CoCrFeMnNi high-entropy alloy: an atomistic simulation study *Npj Comput. Mater.* **4** 1
[33] Berendsen H J, Postma J V, van Gunsteren W F, DiNola A and Haak J 1984 Molecular dynamics with coupling to an external bath *J. Chem. Phys.* **81** 3684–90
[34] Stukowski A 2009 Visualization and analysis of atomistic simulation data with OVITO–the open visualization tool *Modell. Simul. Mater. Sci. Eng.* **18** 015012
[35] Stukowski A, Bulatov V V and Arsenlis A 2012 Automated identification and indexing of dislocations in crystal interfaces *Modell. Simul. Mater. Sci. Eng.* **20** 085007
[36] Schäublin* R, Yao Z, Baluc N and Victoria M 2005 Irradiation-induced stacking fault tetrahedra in fcc metals *Philos. Mag.* **85** 769–77
[37] Granberg F, Djurabekova F, Levo E and Nordlund K 2017 Damage buildup and edge dislocation mobility in equiatomic multicomponent alloys *Nucl. Instrum. Methods Phys. Res. Sect.* B **393** 114–7
[38] Tsai K-Y, Tsai M-H and Yeh J-W 2013 Sluggish diffusion in Co–Cr–Fe–Mn–Ni high-entropy alloys *Acta. Mater.* **61** 4887–97
[39] Wang Z, Fang Q, Li J, Liu B and Liu Y 2018 Effect of lattice distortion on solid solution strengthening of BCC high-entropy alloys *J. Mater. Sci. Technol.* **34** 349–54
[40] Lu C, Jin K, Béland L K, Zhang F, Yang T, Qiao L, Zhang Y, Bei H, Christen H M and Stoller R E 2016 Direct observation of defect range and evolution in ion-irradiated single crystalline Ni and Ni binary alloys *Sci. Rep.* **6** 19994
[41] Arakawa K, Ono K, Isshiki M, Mimura K, Uchikoshi M and Mori H 2007 Observation of the one-dimensional diffusion of nanometer-sized dislocation loops *Science* **318** 956–9
[42] Matsukawa Y and Zinkle S J 2007 One-dimensional fast migration of vacancy clusters in metals *Science* **318** 959–62
[43] Singh B and Foreman A 1992 Production bias and void swelling in the transient regime under cascade damage conditions *Philos. Mag.* A **66** 975–90
[44] Osetsky Y N, Bacon D, Serra A, Singh B and Golubov S 2000 Stability and mobility of defect clusters and dislocation loops in metals *J. Nucl. Mater.* **276** 65–77
[45] Singh B, Golubov S, Trinkaus H, Serra A, Osetsky Y N and Barashev A 1997 Aspects of microstructure evolution under cascade damage conditions *J. Nucl. Mater.* **251** 107–22
[46] Trinkaus H, Singh B and Foreman A 1993 Impact of glissile interstitial loop production in cascades on defect accumulation in the transient *J. Nucl. Mater.* **206** 200–11
[47] Henkelman G, Uberuaga B P and Jonsson H 2000 A climbing image nudged elastic band method for finding saddle points and minimum energy paths *J. Chem. Phys.* **113** 9901–4
[48] Maras E, Trushin O, Stukowski A, Ala-Nissila T and Jonsson H 2016 Global transition path search for dislocation formation in Ge on Si(001) *Comput. Phys. Commun.* **205** 13–21